

# Disorder-driven phase transitions in bosonic fractional quantum Hall liquids

Chao Han<sup>1</sup> and Zhao Liu<sup>1</sup>

<sup>1</sup>*Zhejiang Institute of Modern Physics, Zhejiang University, Hangzhou 310027, China*

(Dated: August 3, 2021)

We investigate the disorder-driven phase transitions in bosonic fractional quantum Hall liquids at filling factors  $f = 1/2$  and  $f = 1$  in the lowest Landau level. We use the evolution of ground-state entanglement entropy, fidelity susceptibility, and Hall conductance with the increasing of disorder strength to identify the underlying phase transitions. The critical disorder strengths obtained from these different quantities are consistent with each other, validating the reliability of our numerical calculations based on exact diagonalization. At  $f = 1/2$ , we observe a clear transition from the bosonic Laughlin state to a trivial insulating phase. At  $f = 1$ , we identify a direct phase transition from the non-Abelian bosonic Moore-Read state to a trivial insulating phase, although some signs of a disorder-induced intermediate fractional quantum Hall phase were recently reported for the  $f = 5/2$  fermionic Moore-Read cousin.

## I. INTRODUCTION

Phase transition is one of the most classical and long-standing problem in condensed matter physics. While Landau's symmetry-breaking theory gains great success in describing phase transitions, the discovery of integer [1] and the more complex, interaction-induced fractional quantum Hall (FQH) effects [2] in two-dimensional electron gases (2DEGs) penetrated by strong magnetic fields clearly indicates the existence of novel topological phases [3] beyond the symmetry-breaking paradigm. Since 1980s, various FQH states, their competing phases, and the transitions between them have been extensively studied [4–23].

Disorder is a ubiquitous ingredient that may drive phase transitions in FQH systems. Although weak disorder is responsible for the characteristic plateaus of Hall conductance when the FQH effects occur, sufficiently strong disorder can destroy FQH phases by closing the spectral gap and mobility gap. Unfortunately, due to the exponentially large Hilbert space of the underlying many-body system as well as the breaking of spatial symmetry, it is challenging to study in the microscopic level how disorder affects FQH phases. In the past decades, only a few numerical studies tackle this problem for fermionic FQH systems [24–29]. By tracking the evolution of the ground-state energy gap, Hall conductance, and entanglement entropy as a function of disorder strength, disorder-driven transitions from Abelian and non-Abelian FQH phases to trivial phases were identified in microscopic models. In particular, for electrons at  $f = 5/2$  whose ground state in the zero-disorder limit is either the non-Abelian fermionic Moore-Read (MR) state or its particle-hole (PH) conjugate anti-MR state [7, 8, 20, 30–32], it was found that enhancing disorder with a finite correlation length might first drive the system into an intermediate FQH phase before completely ruining the topological order [29]. This observation may provide a deep insight into the nature of the mysterious  $f = 5/2$  FQH effect which is still under debate [33–39].

Most studies of FQH physics focus on electrons because of the direct relevance to 2DEGs experiments. However, it has been proposed that bosons in rapidly rotating atomic gases or optical lattices can also form FQH states, where an effective magnetic field is created by rotation or laser beams [40–48]. From the viewpoint of the wavefunction, there is a cor-

respondence between the fermionic and bosonic Read-Rezayi series [40, 49], including the Laughlin [4] and MR states, in which one can obtain a bosonic state from a fermionic one by simply removing a proper Jastrow factor to ensure the correct statistics. This fact immediately raises several interesting questions. How does disorder affect bosonic FQH states? Is the disorder-driven physics for bosonic FQH states similar to the corresponding fermionic cases? In particular, is there a disorder-induced intermediate FQH phase between the bosonic MR state and the trivial strong-disorder limit?

To investigate these problems, in this work we study the effect of disorder for bosons interacting via two-body potentials at filling fractions  $f = 1/2$  and  $f = 1$  in the lowest Landau level (LLL). Similar to the  $f = 1/3$  fermionic case [24, 25, 27], we observe a direct phase transition for  $f = 1/2$  bosons from the bosonic Laughlin state to a trivial insulator. This transition is identified by the special behavior of the ground-state entanglement entropy, fidelity susceptibility, and Hall conductance at the critical disorder strength. However, such a similarity between bosons and fermions seems to be absent for the MR case, in despite of the simple correspondence between the fermionic  $f = 5/2$  and bosonic  $f = 1$  MR wavefunctions. Although a disorder-induced intermediate phase for  $f = 5/2$  fermions might exist [29], we do not find any clear signature of an intermediate phase for  $f = 1$  bosons. Instead, we only identify a single transition from the bosonic MR state to a trivial insulating phase. Promising candidates for the disorder-induced intermediate phase of  $f = 5/2$  fermions include a PH symmetric puddle structure composed of fermionic MR and anti-MR domains [29, 38, 39, 50] and a PH symmetric state [35]. As the usual PH transformation can only be defined for fermions, the absence of an intermediate phase for  $f = 1$  bosons does not contradict with the possible existence of an intermediate PH symmetric phase for  $f = 5/2$  fermions.

The remaining of this paper is organized as follows. In Sec. II, we introduce our model and method in detail, including the many-body Hamiltonian, the disorder model, and the definitions of ground-state entanglement entropy, fidelity susceptibility, and Hall conductance which are used to identify the phase transitions. In Sec. III, we discuss the results at  $f = 1/2$ , which will also benchmark the validity of our method. Then we will move to  $f = 1$  in Sec. IV. Finally, our

conclusions, discussions and outlook are presented in Sec. V.

## II. MODEL AND METHOD

### A. Model

We consider  $N$  interacting bosons of charge  $q$  in a 2D random potential  $U(\mathbf{r})$  on an  $L_1 \times L_2$  rectangular torus penetrated by a uniform perpendicular magnetic field  $B$ . We focus on the strong-field situation such that both the interaction and disorder are small compared with the Landau level spacing. In this case, the system's Hamiltonian is  $\sum_{i < j}^N V(\mathbf{r}_i - \mathbf{r}_j) + \sum_{i=1}^N U(\mathbf{r}_i)$  projected to the LLL, where  $\mathbf{r}_i$  is the coordinate of the  $i$ th boson and  $V(\mathbf{r})$  is the interaction potential.

After using the magnetic length  $\ell_B = \sqrt{\hbar/(qB)}$  as the length unit and choosing the Landau gauge, we can write the LLL single-particle orbitals as

$$\psi_m(\mathbf{r}) = \left( \frac{1}{\sqrt{\pi}L_2} \right)^{\frac{1}{2}} \sum_{n=-\infty}^{+\infty} e^{i\frac{2\pi}{L_2}(m+nN_\phi)y} \times e^{-\frac{1}{2}\left[x - \frac{2\pi}{L_2}(m+nN_\phi)\right]^2}, \quad (1)$$

where  $\mathbf{r} = (x, y)$  is the real-space coordinate,  $N_\phi$  is the number of magnetic flux quanta penetrating the torus, and  $m = 0, \dots, N_\phi - 1$  is the orbital index. As required by the magnetic translational invariance on the torus, we have  $L_1 L_2 = 2\pi N_\phi$  [51]. For simplicity, we choose the isotropic limit with  $L_1 = L_2 = \sqrt{2\pi N_\phi} \equiv L$  throughout this work. In the Fock space spanned by these single-particle orbitals, the LLL-projected Hamiltonian after second quantization takes the form of

$$H = \sum_{m_1, m_2, m_3, m_4=0}^{N_\phi-1} V_{m_1, m_2, m_3, m_4} c_{m_1}^\dagger c_{m_2}^\dagger c_{m_3} c_{m_4} + \sum_{m_1, m_2=0}^{N_\phi-1} U_{m_1, m_2} c_{m_1}^\dagger c_{m_2}, \quad (2)$$

where  $c_m^\dagger$  ( $c_m$ ) creates (annihilates) a boson in the LLL orbital  $m$ , and the interaction and disorder matrix elements are

$$V_{\{m_i\}} = \frac{1}{2L_1 L_2} \delta_{m_1+m_2, m_3+m_4}^{\text{mod } N_\phi} \sum_{s, t=-\infty}^{+\infty} \delta_{t, m_1-m_4}^{\text{mod } N_\phi} V_{\mathbf{q}} \times e^{-\frac{1}{2}|\mathbf{q}|^2} e^{i\frac{2\pi s}{N_\phi}(m_1-m_3)} \quad (3)$$

and

$$U_{\{m_i\}} = \sum_{s, t=-\infty}^{+\infty} \delta_{t, m_1-m_2}^{\text{mod } N_\phi} U_{\mathbf{q}} e^{-\frac{1}{4}|\mathbf{q}|^2} e^{i\frac{\pi s}{N_\phi}(2m_1-t)}, \quad (4)$$

respectively. In Eqs. (3) and (4),  $\delta_{i,j}^{\text{mod } N_\phi}$  is the periodic Kronecker delta function with period  $N_\phi$ ,  $\mathbf{q} = (q_x, q_y) = (2\pi s/L_1, 2\pi t/L_2)$  with  $|\mathbf{q}|^2 = q_x^2 + q_y^2$ ,  $V_{\mathbf{q}}$  and  $U_{\mathbf{q}}$  are

the Fourier transforms of  $V(\mathbf{r})$  and  $U(\mathbf{r})$ , respectively. To study the effects of correlated disorder, we use the Gaussian correlated random potential for  $U(\mathbf{r})$ , which satisfies  $\langle U(\mathbf{r})U(\mathbf{r}') \rangle = \frac{W^2}{2\pi\xi^2} e^{-|\mathbf{r}-\mathbf{r}'|^2/2\xi^2}$  and  $\langle U_{\mathbf{q}}U_{\mathbf{q}'} \rangle = \frac{W^2}{2\pi N_\phi} \delta_{\mathbf{q}, -\mathbf{q}'} e^{-q^2\xi^2/2}$ , where  $\xi$  is the characteristic correlation length,  $W$  is the disorder strength, and  $\langle \dots \rangle$  represents the sample average. If  $\xi = 0$ , we return to the Gaussian white noise. When averaging over  $N_s$  samples, we estimate the error bar of quantity  $A$  by  $\sqrt{(\langle A^2 \rangle - \langle A \rangle^2)/(N_s - 1)}$ .

### B. Entanglement entropy

Topologically ordered phases are characterized by the underlying pattern of quantum entanglement [52–54]. Previous works have found that the ground-state entanglement entropy and its derivative with respect to the disorder strength provide sharp signatures of the disorder-driven phase transitions in FQH systems [27–29]. Here we will apply this diagnosis to bosonic systems. For all cases that we consider, the system at zero and weak disorder is in a topological FQH phase (the bosonic Laughlin phase at  $f = 1/2$  and the bosonic MR phase at  $f = 1$ ) with a well defined manifold consisting of  $D$  approximately degenerate ground states, which are separated by a finite energy gap from other highly excited states. This ground-state degeneracy is a character of the underlying FQH topological order [55]. Therefore, it is natural to extract the entanglement entropy from this ground-state manifold at weak disorder. For consistency, we will always choose the lowest  $D$  eigenstates  $|\Psi_{i=1, \dots, D}\rangle$  of the many-body Hamiltonian Eq. (2) as the ground-state manifold and calculate its entanglement entropy at all disorder strengths, even if the quasi-degeneracy among states in this manifold disappears after the FQH phase is destroyed by strong disorder.

Having defined the ground-state manifold, we divide the whole system into two subsystems  $A$  and  $B$  to calculate the entanglement entropy between them. We consider two kinds of half-half bipartition: (i) the orbital cut [56], for which  $A$  consists of orbitals  $m = 0, \dots, \lceil N_\phi/2 \rceil - 1$  while  $B$  consists of the remaining orbitals, respectively, where  $\lceil a \rceil$  is the integer part of  $a$ ; (ii) the real-space cut [57, 58], for which  $A$  is the region with  $x \in [0, L_1/2]$ ,  $y \in [0, L_2]$  and  $B$  is the complement of  $A$ . The entanglement entropy between  $A$  and  $B$  can be measured by the von Neumann entropy  $S(\rho) = -\text{Tr} \rho_A \ln \rho_A$ , where  $\rho$  is the density matrix of the ground-state manifold and  $\rho_A = \text{Tr}_B \rho$  is the reduced density matrix of part  $A$ . Here  $\rho$  can be chosen as either the average over all states in the ground-state manifold, i.e.,  $\bar{\rho} = \frac{1}{D} \sum_{i=1}^D |\Psi_i\rangle \langle \Psi_i|$ , or a single state  $\rho_i = |\Psi_i\rangle \langle \Psi_i|$ . These two choices correspond to the entanglement entropy  $S(\bar{\rho})$  and  $\bar{S} = \frac{1}{D} \sum_{i=1}^D S(\rho_i)$ , respectively. Both  $S(\bar{\rho})$  and  $\bar{S}$  include the contributions of all  $|\Psi_i\rangle$ 's, thus minimizing the finite-size effect. We have checked that they give similar results, but  $\bar{S}$  suffers from larger finite-size effects. Therefore we will discuss based on the results of  $S(\bar{\rho})$  in what follows.

### C. Fidelity susceptibility

We will also use the ground-state fidelity and fidelity susceptibility to analyze the disorder-driven phase transitions. Fidelity is originally the overlap function between two ground states obtained for two different values of parameters in the Hamiltonian [59]. In our case, it can be generalized to the total overlap between two ground-state manifolds at disorder strength  $W$  and  $W + \Delta W$ , i.e.,

$$F(W) = \left( \frac{1}{D} \sum_{i,j=1}^D |\langle \Psi_i(W) | \Psi_j(W + \Delta W) \rangle|^2 \right)^{1/2}. \quad (5)$$

Since the fidelity measures the similarity between states, the change in the ground-state manifold around the phase transition should be reflected by a dramatic drop of the fidelity across the critical point. A closely related quantity is the fidelity susceptibility defined as

$$\chi(W) = \lim_{\Delta W \rightarrow 0} \frac{-2 \ln F(W)}{\Delta W^2}, \quad (6)$$

which should show a sharp peak diverging with the increasing system size at the phase transition and can describe the universality class of the transition [60, 61].

### D. Hall conductance

The Hall conductance  $\sigma_H$  can unambiguously distinguish FQH phases with nonzero quantized  $\sigma_H$  from insulating phases with  $\sigma_H = 0$  that could exist at strong disorder [24, 25]. After imposing the twisted boundary condition  $\mathcal{T}_\mu \psi_m(\mathbf{r}) = e^{i\theta_\mu} \psi_m(\mathbf{r})$  on the single-particle orbitals Eq. (1), where  $\mathcal{T}_\mu$  is the magnetic translation operator [51] in the  $\mu = x, y$  direction and  $\theta_\mu$  is the boundary phase, we can express the Hall conductance contributed by  $|\Psi_j\rangle$  in the ground-state manifold as  $\sigma_H(j) = C_j q^2/h$ , with

$$C_j = \frac{i}{2\pi} \iint_0^{2\pi} d\theta_x d\theta_y \left( \left\langle \frac{\partial \Psi_j}{\partial \theta_x} \middle| \frac{\partial \Psi_j}{\partial \theta_y} \right\rangle - \left\langle \frac{\partial \Psi_j}{\partial \theta_y} \middle| \frac{\partial \Psi_j}{\partial \theta_x} \right\rangle \right) \quad (7)$$

called the many-body Chern number of  $|\Psi_j\rangle$  [62]. Numerically, we separate the  $\theta_x - \theta_y$  space into dense meshes and calculate the sum of the accumulated Berry phase along the edges of each mesh (divided by  $2\pi$ ) for each state in the ground-state manifold to get  $C_j$ . Then we compute the total many-body Chern number  $C = \sum_{j=1}^D C_j$ , whose associated Hall conductance is  $\sigma_H = Cq^2/h$ .

## III. $f = 1/2$ BOSONIC LAUGHLIN FILLING

Let us first study the disorder driven phase transitions of the  $f = 1/2$  bosons to examine the validity of the diagnoses proposed in Secs. II B, II C and II D. We assume that the bosons interact via the two-body contact potential with constant  $V_q$

in Eq. (3). In this case, the ground state in the absence of disorder is the model bosonic Laughlin state which is exactly two-fold degenerate. For the disorder term Eq. (4), we first consider the Gaussian white noise. One can imagine that the ground state stays in the bosonic Laughlin phase when the disorder is weak, but enters an insulating phase at strong disorder with all bosons pinned at the minimum of the disorder potential. Therefore, at least one phase transition must occur at an intermediate disorder strength.

To identify the phase transition, we measure the orbital-cut entanglement entropy (OEE),  $S^o(\bar{\rho})$ , as a function of disorder strength. At each  $W$ , we consider different disorder configurations and calculate the sample-averaged OEE  $\langle S^o(\bar{\rho}) \rangle$ . Unlike the fermionic cousin at  $f = 1/3$  where  $\langle S^o(\bar{\rho}) \rangle$  monotonically decreases with the increasing of  $W$  [27, 28], for  $f = 1/2$  bosons we find that  $\langle S^o(\bar{\rho}) \rangle$  first grows then decays with increasing  $W$  [Fig. 1(a)]. A peak of  $\langle S^o(\bar{\rho}) \rangle$  develops near  $W = 0.7$  for all system sizes, which seems to indicate a phase transition at  $W \approx 0.7$ .

We further locate the critical point  $W_c$  and extract the critical exponent  $\nu$  of the correlation length via a scaling analysis of the OEE. As the OEE evolves smoothly with the disorder strength, we expect a continuous phase transition at  $W_c$ , with the correlation length

$$\lambda \propto |W - W_c|^{-\nu}$$

near the critical point. Considering that the entanglement entropy obeys the area law, we argue the scaling form

$$S^o(W) - S^o(W_c) \propto Lg[L^{\frac{1}{\nu}}(W - W_c)] \quad (8)$$

for the OEE, where  $g$  is a universal function. By plotting the linear density of the OEE  $[S^o(W) - S^o(W_c)]/L$  versus  $L^{\frac{1}{\nu}}(W - W_c)$ , we find that all data points in Fig. 1(a) (except those of the smallest system size  $N = 4$ ) collapse onto a single curve when we choose  $W_c \approx 0.7 \pm 0.05$  and  $\nu \approx 0.6$  [Fig. 1(c)]. Such a scaling analysis provides a convincing indication of a phase transition at  $W_c \approx 0.7 \pm 0.05$ . Note that the critical exponent  $\nu$  obtained here is close to the value for  $f = 1/3$  fermions [27].

Compared with the entanglement entropy itself, its derivative with respect to the disorder strength may provide a sharper fingerprint of the underlying phase transition [27, 28]. We approximate  $dS^o(\bar{\rho})/dW$  in each sample as  $[S^o(\bar{\rho})|_{W+\Delta W} - S^o(\bar{\rho})|_W]/\Delta W$  with  $\Delta W = 0.001W$ , where  $S^o(\bar{\rho})|_{W+\Delta W}$  is evaluated by only changing the magnitude of  $W$  by a small percentage but keeping the disorder configuration fixed. The sample-averaged result is shown in Fig. 1(b). We observe one peak and one valley in  $\langle dS^o(\bar{\rho})/dW \rangle$ , which occur when  $\langle S^o(\bar{\rho}) \rangle$  grows and decays with increasing  $W$ , respectively. The magnitudes of both the peak and valley grow with increasing system size. While it is difficult to confirm by our exact-diagonalization calculations for relatively small systems, we may expect that the peak and valley both move to the critical  $W_c$  and their magnitudes diverge in the thermodynamic limit. In this case,  $\langle dS^o(\bar{\rho})/dW \rangle$  goes to positive (negative) infinity when  $W \rightarrow W_c$  from the left (right) side, which is a sharp signature of the phase transition. For finite systems, such divergence to positive and

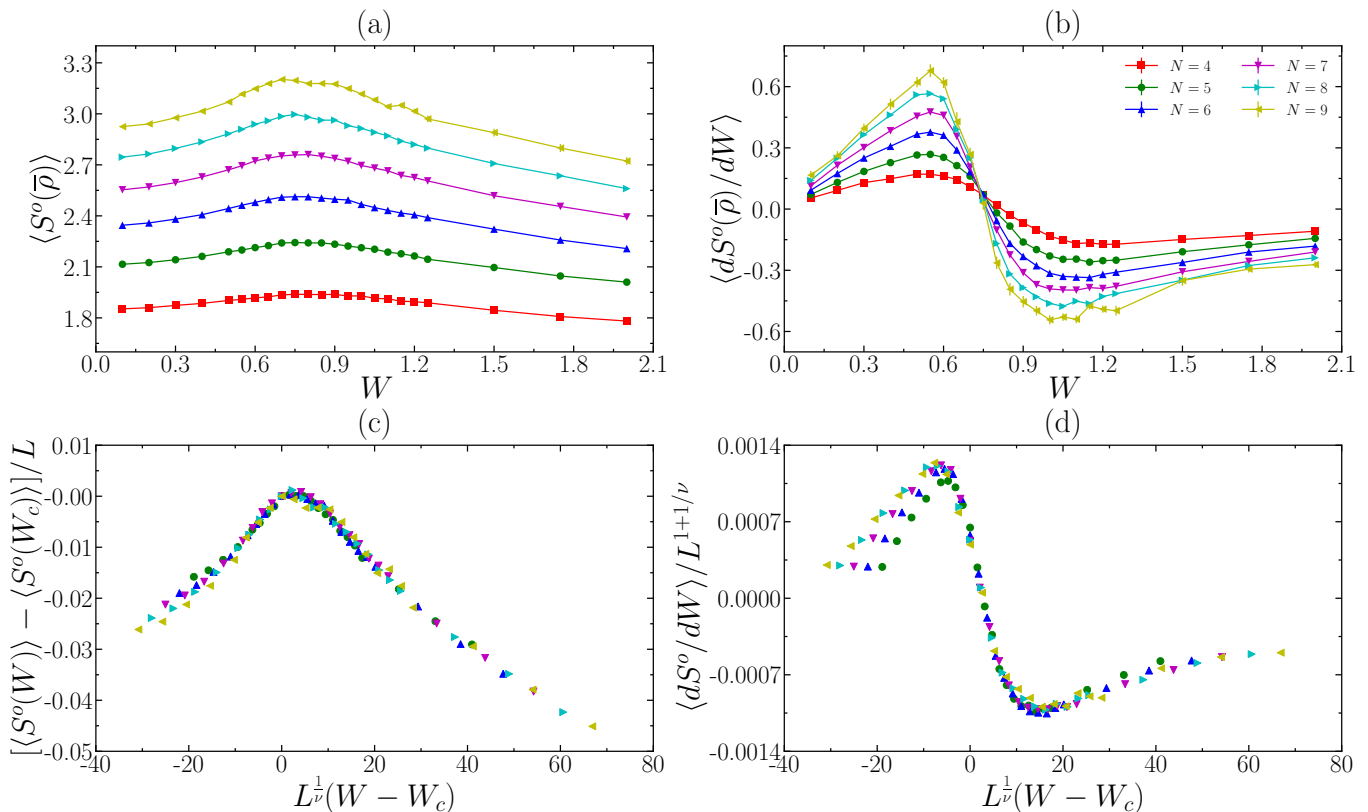


FIG. 1. The orbital-cut entanglement entropy  $S^o(\bar{\rho})$  for  $N = 4 - 9$  bosons at  $f = 1/2$ . Disorder is modeled by the Gaussian white noise. (a)  $\langle S^o(\bar{\rho}) \rangle$  versus  $W$ . (b)  $\langle dS^o(\bar{\rho})/dW \rangle$  versus  $W$ . For the finite-size scaling analysis of  $\langle S^o(W) \rangle$  and  $\langle dS^o/dW \rangle$ , we plot  $[\langle S^o(W) \rangle - \langle S^o(W_c) \rangle]/L$  and  $\langle dS^o/dW \rangle/L^{1+1/\nu}$  versus  $L^{1/\nu}(W - W_c)$  in (c) and (d), respectively, where we use  $W_c = 0.7$  and  $\nu = 0.6$  and neglect the smallest system size  $N = 4$ . We average over 10000 samples for  $N = 4 - 7$ , 3500 samples for  $N = 8$ , and 700 samples for  $N = 9$ . Markers in (a)-(d) with the same color refer to the same system size.

negative infinity are replaced by the peak and valley, respectively. Naively we can estimate  $W_c$  as the position where  $\langle dS^o(\bar{\rho})/dW \rangle \approx 0$ , which again gives  $W_c \approx 0.7$ . Moreover, according to Eq. (8), we suggest the scaling form

$$dS^o(W)/dW \propto L^{1+1/\nu} g'[L^{1/\nu}(W - W_c)] \quad (9)$$

to the entropy derivative, where  $g'$  means derivative of the function  $g$ . In Fig. 1(d), we plot  $\langle dS^o(W)/dW \rangle/L^{1+1/\nu}$  as a function of  $L^{1/\nu}(W - W_c)$  for  $W_c = 0.7$  and  $\nu = 0.6$ . Indeed, all data points in Fig. 1(b) (except those of the smallest system size  $N = 4$ ) collapse to a single curve near the critical point.

At the first glance, the non-monotonic behavior of the orbital-cut entanglement entropy in Fig. 1(a) seems counter-intuitive. With the increasing of the disorder strength, bosons are more likely trapped at the minima of the disorder potential, thus we would expect weaker real-space entanglement between different regions of the system. Since the OEE is often argued to be a reasonable, approximated measure of the real-space entanglement between two subregions of the system due to the Gaussian localization of LLL orbitals [56, 63], one may expect a monotonically decaying OEE, which is nevertheless contrary to our numerical observation that the OEE evolves non-monotonically with the disorder strength. We attribute

this discrepancy to the imprecise capture of the real-space entanglement by the orbital cut – all LLL orbitals have nonzero support across the whole torus, so the orbital cut cannot precisely match the true real-space cut [57, 58]. This mismatch between orbital-cut and real-space entanglement may be more obvious for bosons due to their multiple occupation in each LLL orbital. Indeed, we did not observe the non-monotonic behavior of the OEE for fermions in previous works [27, 28].

In Fig. 2(a), we show the real-space-cut entanglement entropy (REE)  $S^r(\bar{\rho})$  obtained by a true real-space bipartition of the system instead of an orbital cut. Unlike  $\langle S^o(\bar{\rho}) \rangle$ ,  $\langle S^r(\bar{\rho}) \rangle$  indeed monotonically decays with increasing disorder strength, which is consistent with the picture that bosons are trapped at minima of the disorder potential such that the REE becomes smaller. The derivative of  $\langle S^r(\bar{\rho}) \rangle$  with respect to the disorder strength exhibits a single minimum which gets deeper and flows to smaller  $W$  for larger system sizes [Fig. 2 (b)]. Although we can only calculate the REE for at most six electrons due to the larger computational cost than that for the OEE [57, 58], we still try a linear fitting of the minimum position of  $\langle dS^r(\bar{\rho})/dW \rangle$  versus  $1/N$  and obtain  $W_c \approx 0.78$  in the thermodynamic limit, which is consistent with the critical point indicated by the OEE.

The diagnoses above based on entanglement measures sug-

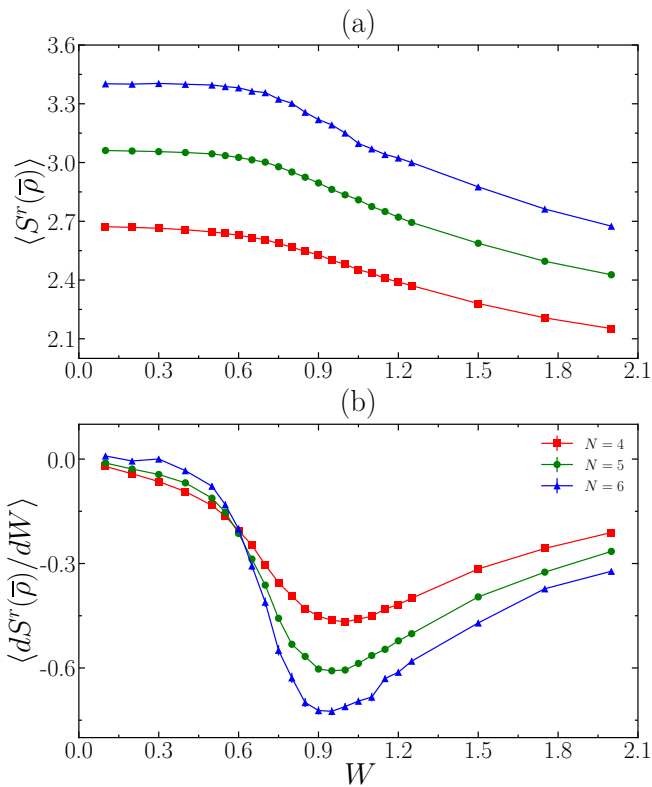


FIG. 2. (a) The sample averaged real-space-cut entanglement entropy  $\langle S^r(\bar{\rho}) \rangle$  and (b) the entropy derivative  $\langle dS^r(\bar{\rho})/dW \rangle$  versus  $W$  for  $N = 4 - 6$  bosons at  $f = 1/2$ . Disorder is modeled by the Gaussian white noise. We average over 10000 samples for  $N = 4 - 5$  and 1500 samples for  $N = 6$ . Markers in (a) and (b) with the same color refer to the same system size.

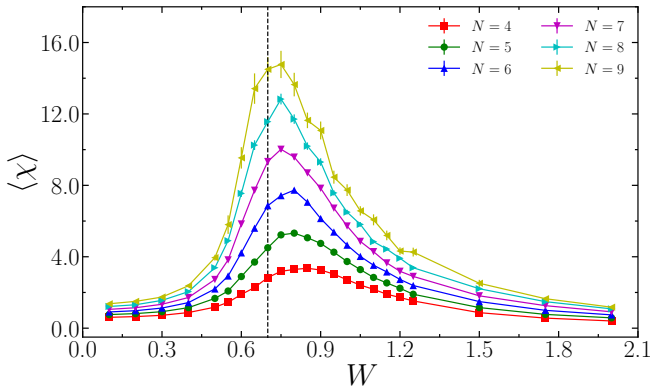


FIG. 3. The sample-averaged fidelity susceptibility  $\langle \chi(W) \rangle$  versus  $W$  for  $N = 4 - 9$  bosons at  $f = 1/2$ . Disorder is modeled by the Gaussian white noise. We average over 10000 samples for  $N = 4 - 7$ , 3500 samples for  $N = 8$ , and 700 samples for  $N = 9$ . The vertical dashed line indicates  $W = 0.7$ , which is the critical disorder strength extracted from the entanglement quantities in Fig. 1.

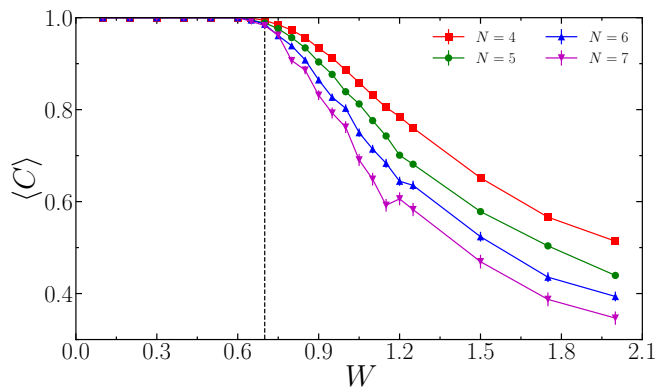


FIG. 4. The sample-averaged many-body Chern number  $\langle C \rangle$  versus  $W$  for  $N = 4 - 7$  bosons at  $f = 1/2$ . Disorder is modeled by the Gaussian white noise. We average over 10000 samples for  $N = 4 - 5$ , 3000 samples for  $N = 6$ , and 1500 samples for  $N = 7$ . The vertical dashed line indicates  $W = 0.7$ , which is the critical disorder strength extracted from the entanglement quantities in Fig. 1.

gest a single phase transition with the increasing of  $W$ . To confirm this, we look for the clue of the phase transition directly at the wave-function level. At each  $W$ , we fix the disorder configuration and change  $W$  by  $\Delta W = 0.001W$  to evaluate the fidelity  $F(W)$  in Eq. (5). Then the fidelity susceptibility  $\chi(W)$  is obtained by Eq. (6), which is further averaged over different disorder configurations. We find a single pronounced maximum in  $\chi(W)$  which gets higher for larger system sizes and probably diverges in the thermodynamic limit (Fig. 3). Such a single peak indicates a single abrupt change of the wave function, i.e., a single phase transition. The location of the peak for the largest three system sizes gives a rough estimate of  $W_c \approx 0.75$ , agreeing with the prediction of the entanglement analysis.

In the end, we track the evolution of the many-body Chern number  $C$  of the ground-state manifold as a function of disorder strength, which can unambiguously distinguish trivial insulators from FQH states. In the Laughlin phase, we should have  $C = 1$ , while we expect  $C = 0$  in the insulating phase. For each disorder configuration, we twist the boundary conditions and evaluate  $C$  by Eq. (7). Then we average  $C$  over various disorder configurations. Indeed, we observe  $\langle C \rangle = 1$  for weak disorder strengths (Fig. 4). A decaying of  $\langle C \rangle$  starts at  $W \approx 0.7$ , signaling the collapse of the Laughlin phase. The drop of  $\langle C \rangle$  becomes steeper for larger system sizes, tending towards a step function in the thermodynamic limit. Note that this critical disorder strength obtained from the many-body Chern number is consistent with the values extracted from the entanglement analysis and fidelity susceptibility, thus validating the reliability of all these diagnoses.

Beside the Gaussian white noise, we have also checked the Gaussian correlated random potential with nonzero correlation length  $\xi$  for  $f = 1/2$  contact-interacting bosons and obtain similar results (not shown here for avoiding repetition).

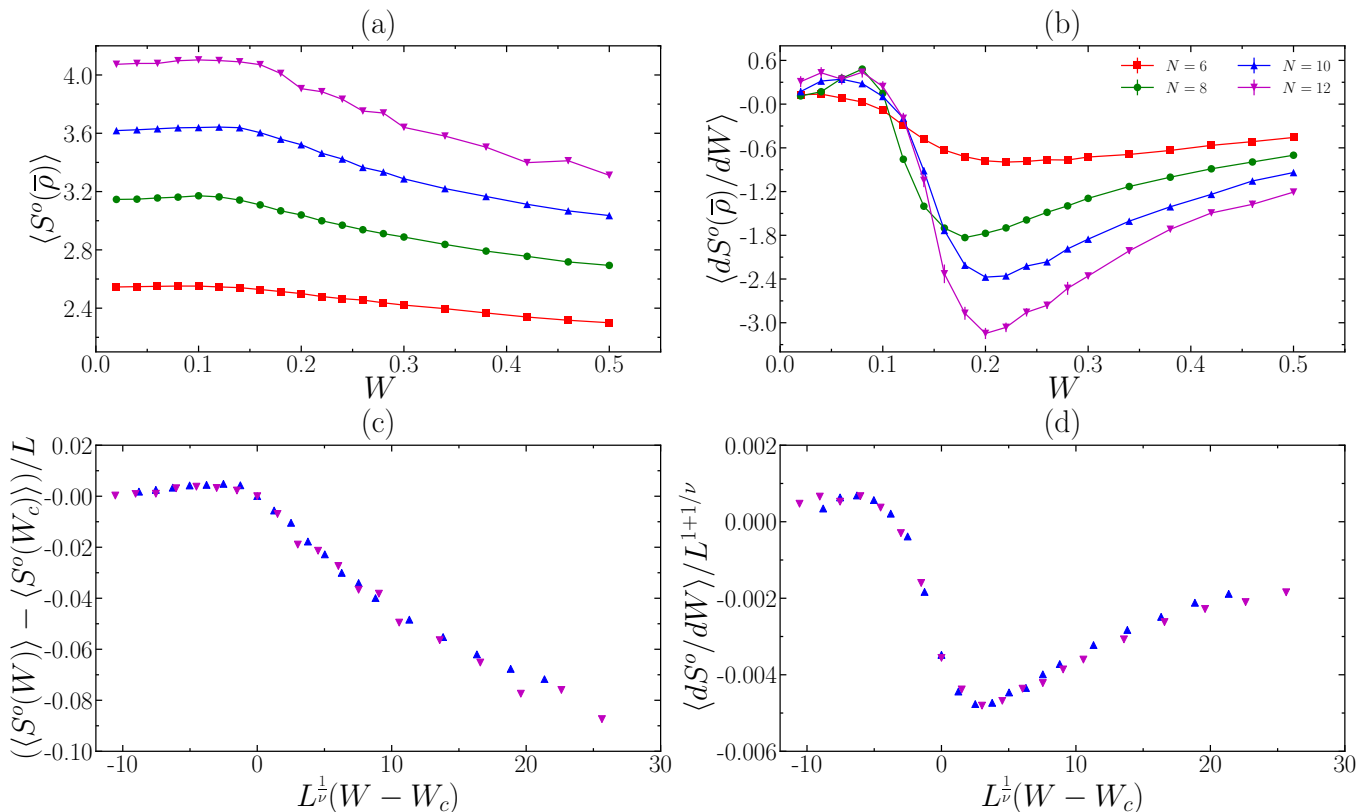


FIG. 5. The orbital-cut entanglement entropy  $S^\circ(\bar{\rho})$  for even  $N = 6 - 12$  bosons at  $f = 1$ . Disorder is modeled by the Gaussian white noise. (a)  $\langle S^\circ(\bar{\rho}) \rangle$  versus  $W$ . (b)  $\langle dS^\circ(\bar{\rho})/dW \rangle$  versus  $W$ . For the finite-size scaling analysis of  $\langle S^\circ(W) \rangle$  and  $\langle dS^\circ/dW \rangle$ , we plot  $[\langle S^\circ(W) \rangle - \langle S^\circ(W_c) \rangle]/L$  and  $\langle dS^\circ/dW \rangle / L^{1+1/\nu}$  versus  $L^{1/\nu}(W - W_c)$  in (c) and (d), respectively, where we use  $W_c = 0.16$  and  $\nu = 0.5$ . We average 10000 samples for  $N = 6$  and 8, 2000 samples for  $N = 10$ , and 500 samples for  $N = 12$ . Markers in (a)-(d) with the same color refer to the same system size.

#### IV. $f = 1$ BOSONIC MOORE-READ FILLING

Having diagnosed the disorder-driven collapse of the  $f = 1/2$  bosonic Laughlin state, we now study the fate of the  $f = 1$  bosonic MR state in the presence of disorder. Before considering the effect of disorder, we need to first establish a bosonic MR phase stabilized by a two-body interaction in the zero-disorder limit. The model bosonic MR state is the exact zero-energy ground state of the three-body contact interaction for even number of bosons and is three-fold degenerate on the torus in the  $\mathbf{K} = (0, 0)$ ,  $\mathbf{K} = (0, N/2)$ , and  $\mathbf{K} = (N/2, 0)$  momentum sectors [64], respectively. Therefore, we will look for a two-body interaction whose lowest three eigenstates are (i) in the same momentum sectors as the model MR states; (ii) approximately three-fold degenerate; and (iii) close to the model MR states.

To achieve this goal, we consider three candidate interactions: the contact interaction, the pure Coulomb interaction, and the Coulomb interaction corrected by a finite layer thickness (due to the quasi-2D nature of the system) [65, 66]. For these interactions, we find the lowest three eigenstates are always in the same momentum sectors as the model bosonic MR state. We then define the ground-state energy gap  $\Delta$  (the ground-state splitting  $\delta$ ) as the energy difference be-

tween the third and the fourth (the first and the third) lowest eigenstate. For each of the three interactions, we calculate  $\Delta/\delta$ , which measures the quality of the degeneracy between the lowest three eigenstates, and the total overlap  $\mathcal{O} = \sum_{i=1}^3 |\langle \Psi_i | \Psi_i^{\text{MR}} \rangle|^2 / 3$  between the lowest three eigenstates  $|\Psi_i\rangle$  and the model bosonic MR states  $|\Psi_i^{\text{MR}}\rangle$ . As shown in Table I, the Coulomb interaction corrected by a finite layer thickness supports the best three-fold ground-state degeneracy and the ground states are the closest to the model bosonic MR state. We hence choose this interaction in what follows and set the typical layer thickness as  $w = 4\ell_B$  [66]. However, we note that the energy scales  $\Delta$  and  $\delta$  still fluctuate with the system size in this case, which may make the disorder strength required to destroy the bosonic MR state also strongly varying with the system size for small systems.

Now we switch on the disorder and study its effect on the bosonic MR state stabilized by the corrected Coulomb interaction. One can imagine that the system must enter an insulating phase at sufficiently strong disorder as all bosons are pinned at the minimum of the disorder potential. Therefore, we expect at least one phase transition from the bosonic MR state to an insulating phase. Note that for  $f = 5/2$  fermions the fermionic MR state is ultimately replaced by a composite fermion liquid [29]. This difference is due to the different

TABLE I. The ratios between the ground-state energy gap  $\Delta$  and the ground-state splitting  $\delta$  at zero disorder for  $f = 1$  bosons with the contact interaction, the Coulomb interaction, and the Coulomb interaction corrected by a finite layer thickness  $w = 4\ell_B$ , respectively. For all interactions, the ground-state manifold contains the lowest three eigenstates which are always in the same momentum sectors as the model bosonic MR state. The total overlaps  $\mathcal{O}$  between the ground-state manifold and the model bosonic MR states are also given.

|          | $V_0$           |               | pure Coulomb    |               |                 |               | Coulomb $w = 4\ell_B$ |               |
|----------|-----------------|---------------|-----------------|---------------|-----------------|---------------|-----------------------|---------------|
|          | $\Delta/\delta$ | $\mathcal{O}$ | $\Delta/\delta$ | $\mathcal{O}$ | $\Delta/\delta$ | $\mathcal{O}$ | $\Delta/\delta$       | $\mathcal{O}$ |
| $N = 6$  | 2.5377          | 0.9582        | 2.1650          | 0.9645        | 2.1279          | 0.9648        |                       |               |
| $N = 8$  | 0.4261          | 0.8939        | 1.2231          | 0.9491        | 2.0896          | 0.9676        |                       |               |
| $N = 10$ | 0.6755          | 0.8968        | 1.9949          | 0.9296        | 3.1334          | 0.9412        |                       |               |
| $N = 12$ | 3.7860          | 0.8080        | 7.8853          | 0.8823        | 10.488          | 0.9109        |                       |               |
| $N = 14$ | 2.2126          | 0.8152        | 3.6643          | 0.8770        | 4.9111          | 0.9018        |                       |               |
| $N = 16$ | 7.3220          | 0.7215        | 23.414          | 0.8318        | 47.486          | 0.8749        |                       |               |

statistics between bosons and fermions. In the presence of disorder, each Landau level is broadened into a Landau band and all single-particle states except those at the band center are localized. While in the strong-disorder limit (zero interaction) all bosons can pile in a single localized single-particle state with the lowest energy,  $f = 5/2$  fermions must occupy half of the single-particle states in the second Landau band including the delocalized states at the band center as two fermions cannot occupy the same single-particle state.

To proceed, we first model disorder by the Gaussian white noise. Similar to the Laughlin case, the OEE  $\langle S^o(\bar{\rho}) \rangle$  first increases then decreases with the increasing of  $W$  for all system sizes [Fig. 5(a)], leading to a peak and a valley in the entropy derivative  $\langle dS^o(\bar{\rho})/dW \rangle$  [Fig. 5(b)], while the REE decays monotonically (not shown here). We believe that the critical point  $W_c$  can be identified by maximum of the OEE, and the OEE derivative diverges to positive (negative) infinity on the left (right) side of the critical point in the thermodynamic limit. However, as hinted by the energy scales in Table I which fluctuate with the system size, the OEE data in Fig. 5, especially the entropy derivative suffer from a much stronger finite-size effect than the  $f = 1/2$  Laughlin case. As a result, we use the data of the largest two system sizes  $N = 10$  and  $N = 12$  to do the scaling analysis to extract  $W_c$ . We apply the scaling forms Eqs. (8) and (9) to  $\langle S^o(\bar{\rho}) \rangle$  and  $\langle dS^o(\bar{\rho})/dW \rangle$ , respectively. With the rescaled variables, we find that all data points almost locate on a single curve with  $W_c \approx 0.16$  and  $\nu \approx 0.5$  [Figs. 5(c) and 5(d)].

To check the critical  $W$  extracted from the entanglement quantities, we calculate the fidelity susceptibility  $\langle \chi(W) \rangle$  (Fig. 6). Similar to the Laughlin case, all  $\langle \chi(W) \rangle$  curves exhibit a pronounced maximum which gets higher for larger system size. While the position of the peak varies for small systems, it is located at  $W \approx 0.16$  for the largest system  $N = 12$ , which matches  $W_c$  extracted from the OEE.

The similar behavior of the OEE to the  $f = 1/2$  Laughlin case and the single peak in the fidelity susceptibility suggest a direct phase transition from the bosonic MR state to an

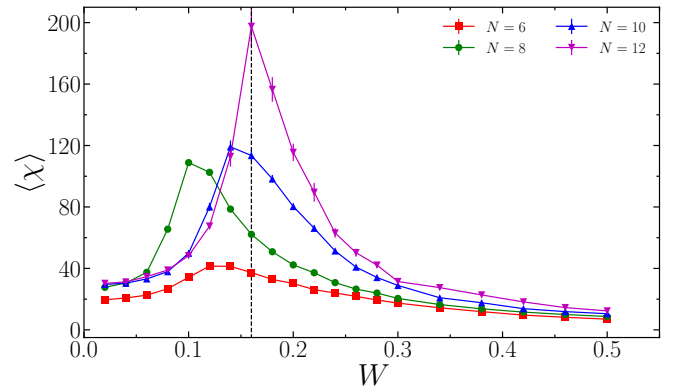


FIG. 6. The sample-averaged fidelity susceptibility  $\langle \chi(W) \rangle$  for even  $N = 6 - 12$  bosons at  $f = 1$ . Disorder is modeled by the Gaussian white noise. We average 10000 samples for  $N = 6$  and 8, 2000 samples for  $N = 10$ , and 500 samples for  $N = 12$ . The vertical dashed line indicates  $W = 0.16$ , which is the critical disorder strength extracted from the entanglement quantities in Fig. 5.

insulating phase when the disorder is modeled by the Gaussian white noise. Motivated by the intriguing observation that an intermediate FQH phase might exist for the  $f = 5/2$  fermionic MR state subjected to disorder with a finite correlation length  $\xi$  [29], we repeat the studies in Figs. 5 and 6 by using the Gaussian correlated random potential with nonzero  $\xi$ . We consider  $\xi/\ell_B = 0.5 - 2$ , for which a disorder-induced intermediate FQH phase seems to exist for  $f = 5/2$  fermions [29]. However, for  $f = 1$  bosons, we cannot see any clear signature of an intermediate phase within this range of  $\xi$ . The results for  $\xi = 0.5\ell_B$  and  $\xi = \ell_B$  are shown in Fig. 7. In these cases, the OEE and the fidelity susceptibility look qualitatively similar to the  $\xi = 0$  case (i.e., the Gaussian white noise). While the curves at  $\xi > 0$  are stretched compared to the  $\xi = 0$  case such that the critical  $W$  moves to larger values [Figs. 7(a)-(c), (e)-(g)], we can only observe the signature of a single phase transition, as reflected by the single pronounced peak in the fidelity susceptibility [Figs. 7(c), (g)]. This is also true for larger  $\xi$  despite of stronger finite-size effects. We also find the many-body Chern number stays at  $\langle C \rangle = 3$  at weak disorder and decays at sufficiently large  $W$  [Figs. 7(d), (h)], which confirms the transition from the bosonic MR state to an insulating phase.

## V. CONCLUSIONS AND DISCUSSIONS

In this paper, we present a systematic exact-diagonalization study of disorder-driven quantum phase transitions for the  $f = 1/2$  and  $f = 1$  bosonic FQH systems. We identify the phase transition by tracking the entanglement entropy, fidelity susceptibility, and many-body Chern number (Hall conductance) of the ground-state manifold as a function of disorder strength. The critical disorder strengths  $W_c$  obtained from different quantities are consistent with each other, validating the reliability of our numerical results. At both  $f = 1/2$  and  $f = 1$ , we identify a single phase transition from the

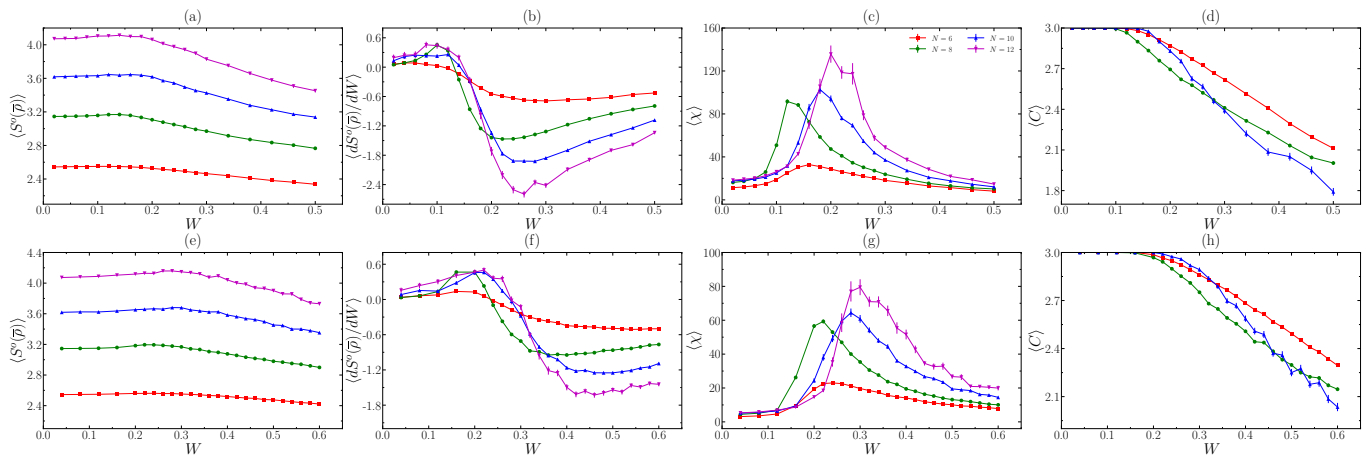


FIG. 7. The sample-averaged orbital-cut entanglement entropy  $\langle S^o(\bar{\rho}) \rangle$ , entropy derivative  $\langle dS^o(\bar{\rho})/dW \rangle$ , fidelity susceptibility  $\langle \chi(W) \rangle$ , and many-body Chern number  $\langle C \rangle$  for even  $N = 6 - 12$  bosons at  $f = 1$ . Disorder is modeled by the Gaussian correlated random potential with  $\xi = 0.5\ell_B$  [top panel, (a)-(d)] and  $\xi = \ell_B$  [bottom panel, (e)-(h)]. In (a)-(c) and (e)-(g), we average 10000 samples for  $N = 6$  and 8, 2000 samples for  $N = 10$ , and 500 samples for  $N = 12$ . Due to the larger computational cost of the many-body Chern number which requires integrating over boundary conditions, we average 10000 samples for  $N = 6$ , 5000 samples for  $N = 8$  and 1000 samples for  $N = 10$  in (d) and (h). Markers in (a)-(h) with the same color refer to the same system size.

FQH state (bosonic Laughlin for  $f = 1/2$  and bosonic MR for  $f = 1$ ) to an insulating phase, no matter the correlation length in the disorder potential is zero or not. While the location of the transition appears to be robust, the critical exponent  $\nu$  of the transition extracted from the finite-size scaling analysis of the OEE data violates the expected Harris-Chayes inequality  $\nu \geq 2/d$  for  $d$ -dimensional disordered systems [67, 68]. Such violation was also observed in fermionic FQH systems [27, 28] and many-body localization transitions [69, 70]. Our results may motivate further studies of the critical exponent of disorder-driven phase transitions in FQH systems by more powerful numerical techniques and experiments.

The fate of the  $f = 1$  bosonic MR state in the presence of disorder looks different from that of the  $f = 5/2$  fermionic MR state. At least in the range of the disorder correlation length considered by us ( $\xi/\ell_B = 0.5 - 2$ ), we observe a direct transition to an insulating phase for the former, while for the latter the system might first enter an intermediate FQH phase before finally becoming a composite-fermion liquid [29]. The suspected intermediate phase in the fermionic case was argued to be a PH symmetric phase described by either the fermionic MR-anti-MR puddle structure [29, 38, 39, 50] or a PH symmetric wavefunction [35]. Since the usual PH transformation is only well-defined for fermions, it is indeed impossible for

bosons to form a PH symmetric intermediate phase induced by disorder. Therefore, our results do not contradict with the existence of a PH symmetric intermediate phase of  $f = 5/2$  fermions. In Ref. [71], a generalized PH transformation is defined for bosons, by which one can construct a bosonic anti-MR state at  $f = 1$ . However, unlike in the fermionic case where the MR and anti-MR states have the same energies for PH symmetric Hamiltonians, this bosonic anti-MR state could have a much higher energy than the bosonic MR state. Indeed, the absence of an intermediate phase in our numerical results seems to suggest that the bosonic anti-MR state is not energetically favored by the realistic Hamiltonian we use.

A future direction following our work could be exploring the disorder effect on bosonic FQH states in lattice systems, i.e. the fractional Chern insulators [72–74]. In that case, the notable differences between a Chern band and the LLL, such as the multi-band structure and high Chern number may host new interesting phenomena.

## ACKNOWLEDGMENTS

We thank Bo Yang, Wei Zhu and Xin Wan for fruitful discussions. This work is supported by the National Natural Science Foundation of China through Grant No. 11974014.

[1] K. v. Klitzing, G. Dorda, and M. Pepper, *Phys. Rev. Lett.* **45**, 494 (1980).  
 [2] D. C. Tsui, H. L. Stormer, and A. C. Gossard, *Phys. Rev. Lett.* **48**, 1559 (1982).  
 [3] X. G. WEN, *International Journal of Modern Physics B* **04**, 239 (1990).  
 [4] R. B. Laughlin, *Phys. Rev. Lett.* **50**, 1395 (1983).

[5] F. D. M. Haldane, *Phys. Rev. Lett.* **51**, 605 (1983).  
 [6] J. K. Jain, *Phys. Rev. Lett.* **63**, 199 (1989).  
 [7] G. Moore and N. Read, *Nuclear Physics B* **360**, 362 (1991).  
 [8] R. H. Morf, *Phys. Rev. Lett.* **80**, 1505 (1998).  
 [9] H. L. Stormer, *Rev. Mod. Phys.* **71**, 875 (1999).  
 [10] I. A. McDonald and F. D. M. Haldane, *Phys. Rev. B* **53**, 15845 (1996).

- [11] E. Ardonne and K. Schoutens, *Phys. Rev. Lett.* **82**, 5096 (1999).
- [12] W. Pan, H. L. Stormer, D. C. Tsui, L. N. Pfeiffer, K. W. Baldwin, and K. W. West, *Phys. Rev. Lett.* **90**, 016801 (2003).
- [13] G. Gervais, L. W. Engel, H. L. Stormer, D. C. Tsui, K. W. Baldwin, K. W. West, and L. N. Pfeiffer, *Phys. Rev. Lett.* **93**, 266804 (2004).
- [14] T. Jolicoeur, *Phys. Rev. Lett.* **99**, 036805 (2007).
- [15] Z. Papić, M. O. Goerbig, N. Regnault, and M. V. Milovanović, *Phys. Rev. B* **82**, 075302 (2010).
- [16] A. C. Archer and J. K. Jain, *Phys. Rev. Lett.* **110**, 246801 (2013).
- [17] S. Geraedts, M. P. Zaletel, Z. Papić, and R. S. K. Mong, *Phys. Rev. B* **91**, 205139 (2015).
- [18] Z. Liu, A. Vaezi, K. Lee, and E.-A. Kim, *Phys. Rev. B* **92**, 081102 (2015).
- [19] M. R. Peterson, Y.-L. Wu, M. Cheng, M. Barkeshli, Z. Wang, and S. Das Sarma, *Phys. Rev. B* **92**, 035103 (2015).
- [20] K. Pakrouski, M. R. Peterson, T. Jolicoeur, V. W. Scarola, C. Nayak, and M. Troyer, *Phys. Rev. X* **5**, 021004 (2015).
- [21] N. Thiebaut, N. Regnault, and M. O. Goerbig, *Phys. Rev. B* **92**, 245401 (2015).
- [22] C. Gils, S. Trebst, A. Kitaev, A. W. W. Ludwig, M. Troyer, and Z. Wang, *Nature Physics* **5**, 834 (2009).
- [23] N. Samkharadze, K. A. Schreiber, G. C. Gardner, M. J. Manfra, E. Fradkin, and G. A. Csáthy, *Nature Physics* **12**, 191 (2016).
- [24] D. N. Sheng, X. Wan, E. H. Rezayi, K. Yang, R. N. Bhatt, and F. D. M. Haldane, *Phys. Rev. Lett.* **90**, 256802 (2003).
- [25] X. Wan, D. N. Sheng, E. H. Rezayi, K. Yang, R. N. Bhatt, and F. D. M. Haldane, *Phys. Rev. B* **72**, 075325 (2005).
- [26] B. A. Friedman, G. C. Levine, and D. Luna, *New Journal of Physics* **13**, 055006 (2011).
- [27] Z. Liu and R. N. Bhatt, *Phys. Rev. Lett.* **117**, 206801 (2016).
- [28] Z. Liu and R. N. Bhatt, *Phys. Rev. B* **96**, 115111 (2017).
- [29] W. Zhu and D. N. Sheng, *Phys. Rev. Lett.* **123**, 056804 (2019).
- [30] E. H. Rezayi and F. D. M. Haldane, *Phys. Rev. Lett.* **84**, 4685 (2000).
- [31] M. R. Peterson, K. Park, and S. Das Sarma, *Phys. Rev. Lett.* **101**, 156803 (2008).
- [32] E. H. Rezayi, *Phys. Rev. Lett.* **119**, 026801 (2017).
- [33] D. T. Son, *Phys. Rev. X* **5**, 031027 (2015).
- [34] X. Wan and K. Yang, *Phys. Rev. B* **93**, 201303 (2016).
- [35] P. T. Zucker and D. E. Feldman, *Phys. Rev. Lett.* **117**, 096802 (2016).
- [36] M. Banerjee, M. Heiblum, V. Umansky, D. E. Feldman, Y. Oreg, and A. Stern, *Nature* **559**, 205 (2018).
- [37] R. V. Mishmash, D. F. Mross, J. Alicea, and O. I. Motrunich, *Phys. Rev. B* **98**, 081107 (2018).
- [38] D. F. Mross, Y. Oreg, A. Stern, G. Margalit, and M. Heiblum, *Phys. Rev. Lett.* **121**, 026801 (2018).
- [39] C. Wang, A. Vishwanath, and B. I. Halperin, *Phys. Rev. B* **98**, 045112 (2018).
- [40] N. R. Cooper, N. K. Wilkin, and J. M. F. Gunn, *Phys. Rev. Lett.* **87**, 120405 (2001).
- [41] N. Regnault and T. Jolicoeur, *Phys. Rev. Lett.* **91**, 030402 (2003).
- [42] E. H. Rezayi, N. Read, and N. R. Cooper, *Phys. Rev. Lett.* **95**, 160404 (2005).
- [43] A. S. Sørensen, E. Demler, and M. D. Lukin, *Phys. Rev. Lett.* **94**, 086803 (2005).
- [44] N. Regnault and T. Jolicoeur, *Phys. Rev. B* **76**, 235324 (2007).
- [45] N. R. Cooper, *Advances in Physics* **57**, 539 (2008).
- [46] A. L. Fetter, *Rev. Mod. Phys.* **81**, 647 (2009).
- [47] G. Möller and N. R. Cooper, *Phys. Rev. Lett.* **103**, 105303 (2009).
- [48] N. R. Cooper and J. Dalibard, *Phys. Rev. Lett.* **110**, 185301 (2013).
- [49] N. Read and E. Rezayi, *Phys. Rev. B* **59**, 8084 (1999).
- [50] B. Lian and J. Wang, *Phys. Rev. B* **97**, 165124 (2018).
- [51] F. D. M. Haldane, *Phys. Rev. Lett.* **55**, 2095 (1985).
- [52] J. Eisert, M. Cramer, and M. B. Plenio, *Rev. Mod. Phys.* **82**, 277 (2010).
- [53] A. Kitaev and J. Preskill, *Phys. Rev. Lett.* **96**, 110404 (2006).
- [54] M. Levin and X.-G. Wen, *Phys. Rev. Lett.* **96**, 110405 (2006).
- [55] X. G. Wen and Q. Niu, *Phys. Rev. B* **41**, 9377 (1990).
- [56] M. Haque, O. Zozulya, and K. Schoutens, *Phys. Rev. Lett.* **98**, 060401 (2007).
- [57] A. Sterdyniak, A. Chandran, N. Regnault, B. A. Bernevig, and P. Bonderson, *Phys. Rev. B* **85**, 125308 (2012).
- [58] J. Dubail, N. Read, and E. H. Rezayi, *Phys. Rev. B* **85**, 115321 (2012).
- [59] P. Zanardi and N. Paunković, *Phys. Rev. E* **74**, 031123 (2006).
- [60] W.-L. You, Y.-W. Li, and S.-J. Gu, *Phys. Rev. E* **76**, 022101 (2007).
- [61] S.-J. Gu, H.-M. Kwok, W.-Q. Ning, and H.-Q. Lin, *Phys. Rev. B* **77**, 245109 (2008).
- [62] Q. Niu, D. J. Thouless, and Y.-S. Wu, *Phys. Rev. B* **31**, 3372 (1985).
- [63] H. Li and F. D. M. Haldane, *Phys. Rev. Lett.* **101**, 010504 (2008).
- [64] C. Repellin, T. Neupert, B. A. Bernevig, and N. Regnault, *Phys. Rev. B* **92**, 115128 (2015).
- [65] M. R. Peterson, T. Jolicoeur, and S. Das Sarma, *Phys. Rev. B* **78**, 155308 (2008).
- [66] M. R. Peterson, T. Jolicoeur, and S. Das Sarma, *Phys. Rev. Lett.* **101**, 016807 (2008).
- [67] A. B. Harris, *Journal of Physics C: Solid State Physics* **7**, 3082 (1974).
- [68] J. T. Chayes, L. Chayes, D. S. Fisher, and T. Spencer, *Phys. Rev. Lett.* **57**, 2999 (1986).
- [69] J. A. Kjäll, J. H. Bardarson, and F. Pollmann, *Phys. Rev. Lett.* **113**, 107204 (2014).
- [70] D. J. Luitz, N. Laflorencie, and F. Alet, *Phys. Rev. B* **91**, 081103 (2015).
- [71] C. Wang and T. Senthil, *Phys. Rev. B* **94**, 245107 (2016).
- [72] S. A. Parameswaran, R. Roy, and S. L. Sondhi, *Comptes Rendus Physique* **14**, 816 (2013).
- [73] E. J. Bergholtz and Z. Liu, *International Journal of Modern Physics B* **27**, 1330017 (2013).
- [74] T. Neupert, C. Chamon, T. Iadecola, L. H. Santos, and C. Mudry, *Physica Scripta* **2015**, 014005 (2015).